

# Whole-Body Control of a Mobile Manipulator for Passive Collaborative Transportation

F. Benzi \* C. Mancus \* C. Secchi \*

\* *Department of Sciences and Methods of Engineering, University of Modena and Reggio Emilia, Italy (e-mail: federico.benzi@unimore.it, cristian.mancus@unimore.it, cristian.secchi@unimore.it)*

---

## Abstract:

Human-robot collaborative tasks foresee interactions between humans and robots with various degrees of complexity. Specifically, for tasks which involve physical contact among the agents, challenges arise in the modelling and control of such interaction. In this paper we propose a control architecture capable of ensuring a flexible and robustly stable physical human-robot interaction, focusing on a collaborative transportation task. The architecture is deployed onto a mobile manipulator, modelled as a whole-body structure, which aids the operator during the transportation of an unwieldy load. Thanks to passivity techniques, the controller adapts its interaction parameters online while preserving robust stability for the overall system, thus experimentally validating the architecture.

*Keywords:* Force and Compliance Control, Adaptive Robot Control, Robust Robot Control, Haptic Interaction, Physical Human-Robot Interaction.

---

## 1. INTRODUCTION

The modern industrial paradigm foresees an increasingly close interaction among humans and robots. This is most strongly manifested in collaborative applications, in which the robot assists or cooperates with the human in order to accomplish a common goal.

During some collaborative tasks, a physical contact between the robot and its surroundings, these being the human or the environment, might take place. This contact can take place either directly onto the surface of the robot, or via the manipulation of a collaboratively held object. In this paper, we focus onto these types of contact, aiming at rendering such interactions both flexible and robust to different environments and parameter variations.

Different approaches in literature have been proposed for a safe and reliable collaborative load transportation. A vastly employed one is to teach the robot the collaborative task by means of programming by demonstration (PbD) Calinon et al. (2009), Gribovskaya et al. (2011), in which the robot learns by encoding the human demonstrations as a task. The encoding process of the task model can be carried out via probabilistic frameworks based on Gaussian Mixture Model (GMM) Calinon et al. (2007) or Hidden Markov Model Hersch et al. (2008). However, except for a certain degree of adaptation during the task execution, the performance of these controllers drop significantly whenever the interaction varies strongly from the demonstrated data, since their principle of operation is based on the local knowledge of the task. Thus, their generalization capabilities and consequently their flexibility are limited, making those non-ideal for dynamic environments. Additionally,

learning-based methods also do not generally include the possibility of additional tasks, such as safety and joint limits control. Finally, processes as task model training and parameters tuning can result time consuming.

Other approaches directly integrate haptic information into an impedance or admittance controller Agravante et al. (2013); Tagliabue et al. (2017) in order for the robot to comply with the external forces acting onto the manipulated object. Impedance and admittance control Siciliano and Villani (2012) are two commonly deployed strategies in interaction control. These controllers ensure compliance of the robot during the interaction phase by enforcing a dynamical behaviour in the form of a mechanical impedance, characterised by desired stiffness, damping and inertia parameters. In this way, the robot can adapt its behaviour according to haptic information and guarantee a stable interaction. In Tagliabue et al. (2017) two Micro Aerial Vehicles (MAVs) perform a collaborative transportation task based on the master-slave paradigm, in which the slave complies to the external force applied by the master to the payload via an admittance controller. The inherent passivity of the dynamics ensures a robustly stable interaction Secchi et al. (2007).

Adapting the dynamic parameters during the interaction can be greatly beneficial for the application, since it allows for an higher flexibility of the behaviour, of peculiar interest for collaborative applications Dimeas and Aspragathos (2016). This is carried out e.g. in Gribovskaya et al. (2011), in which an adaptive impedance is utilised to compensate for unmodeled uncertainties during the collaborative task execution due to the human behaviour. In here, however, there is no formal stability analysis of the adaptive

impedance. In fact, varying online the dynamic parameters may lead to the loss of passivity Ferraguti et al. (2015) and unstable behaviours might be implemented during the human-robot interaction Ferraguti et al. (2019).

The formulation of a provably stable variable admittance controller has been successfully carried out in Secchi and Ferraguti (2019) by means of an optimization framework. The exploitation of energy tanks Ferraguti et al. (2015); Franken et al. (2011) allows to separate passivity from set dynamics, treating the energy flow in the tank as a requirement for the passivation of any desired behaviour.

The architecture was successively augmented in Benzi and Secchi (2021), allowing for the simultaneous execution of multiple additional tasks alongside the passivation of the behaviour. In here, the tasks are encoded by means of Control Barrier Functions (CBFs) Ames et al. (2019) following a procedure akin to Notomista et al. (2020). CBFs have been deployed in robotics in order to constraint the system inside a subset of its state space, thus enforcing constraints onto the behaviour of the robot. Via time-varying CBFs Notomista and Egerstedt (2020) it is also possible to enforce time-varying constraint, which are well suited for safety applications. The control input satisfying the set of constraint can be found as the solution of a convex optimization problem, ensuring the real-time capabilities of the architecture. Nevertheless, only simple robotic arms have been considered so far.

Subsequent evolutions of the architecture are presented in Benzi et al. (2022), in which the control structure is deployed for passively implementing shared autonomy in a multi-robot teleoperation scenario, and in Ferrari et al. (2022) for an effective and seamless human-robot collaboration via a bidirectional communication channel.

In this paper, we aim at deploying the architecture presented in Benzi and Secchi (2021), further augmenting it for achieving the whole body control of the robot, in order to reproduce a collaborative human-robot transportation task in a robustly stable way, while performing additional tasks. This novel approach allows us to overcome the rigidity of standard PbD approaches, ensuring a flexible and adaptable behaviour at all times, while preserving the safety of all the parties involved.

The robot chosen for the application is a custom mobile manipulator, consisting of a differential drive mobile platform with a robotic arm mounted on top, modeled as a whole body system. A similar task was implemented in Nozaki and Murakami (2009), but the arm and the mobile base were modelled separately and the impedance dynamics was fixed.

Thus, the contributions of this paper are:

- A control architecture capable of performing a collaborative human-robot transportation task in a flexible and robust way
- A whole-body kinematic model and control of the robot, capable of considering non-holonomic constraints introduced by the mobile base
- The possibility of implementing multiple tasks alongside the main transportation one

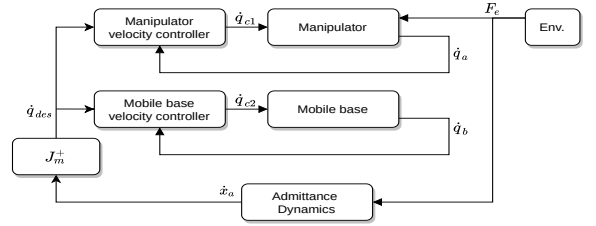


Fig. 1. Whole-body admittance control architecture. We indicate as  $\dot{\mathbf{q}}_{c1}$  and  $\dot{\mathbf{q}}_{c2}$  the setpoint for the velocity controllers of the manipulator and the mobile base respectively.

The paper is organised as follows: in Sec. 2 the main problem addressed in this paper is formulated. In Sec. 3 the whole-body model of the mobile manipulator is laid out. In Sec. 4 the collaborative constraint-oriented control architecture is presented. In Sec. 5 the architecture is experimentally validated and finally in Sec. 6 conclusions are drawn and future work is discussed.

## 2. PROBLEM FORMULATION

Let us consider a velocity controlled mobile manipulator composed of a fully actuated  $n_a$ -DOF manipulator mounted onto a differential drive mobile base, assuming that the low-level controllers of both robots ensure accurate reproduction of a desired velocity profile. We consider the following extended joint space for the robot:

$$\mathbf{q} = \begin{bmatrix} \mathbf{q}_b \\ \mathbf{q}_a \end{bmatrix} \quad (1)$$

in which  $\mathbf{q}_a \in \mathbb{R}^{n_a}$  are the generalized coordinates of the manipulator, while  $\mathbf{q}_b \in \mathbb{R}^{n_b}$  are the angular position of the wheels of the mobile base. We define as  $N = n_a + n_b$  the dimension of the augmented configuration space.

We construct the augmented mapping for the robot

$${}^W \dot{\mathbf{x}}_E = \mathbf{J}_m \dot{\mathbf{q}} \quad (2)$$

relating the end tip velocity w.r.t the world frame  ${}^W \dot{\mathbf{x}}_E \in \mathbb{R}^m$  with the robot velocity in the augmented joint space. We refer to  $\mathbf{J}_m \in \mathbb{R}^{m \times N}$  as the augmented Jacobian.

We can obtain the desired velocity input in the joint space  $\mathbf{u} \in \mathbb{R}^N$  which implements a desired task space velocity  $\dot{\mathbf{x}}_{des}$  as  $\mathbf{u} = \dot{\mathbf{q}}_{des} = \mathbf{J}_m^+ \dot{\mathbf{x}}_{des}$  in which  $\mathbf{J}_m^+ \in \mathbb{R}^{N \times m}$  is the Moore-Penrose pseudo-inverse of the augmented Jacobian.

We finally assume that the human-robot contact takes place via a commonly manipulated object, whose interaction force  $\mathbf{F}_e \in \mathbb{R}^m$  is sensed by a haptic interface. We model the interaction using the whole body admittance controller in Fig. 1, i.e. by integrating the interaction force via the admittance dynamics, synthesizing the admittance velocity  $\dot{\mathbf{x}}_a \in \mathbb{R}^m$ . We can then ensure the reproduction of the admittance dynamics by setting  ${}^W \dot{\mathbf{x}}_E \approx \dot{\mathbf{x}}_{des} \approx \dot{\mathbf{x}}_a$ .

In order to enhance the performance of the controller, we want to vary the admittance parameters according to the perceived intention of the human operator, assisting him during the manipulation of the object at the best of the robot capabilities (see e.g. Ferraguti et al. (2019)). Passivity is however lost if we consider a variable admittance controller, i.e. whose dynamic parameters vary over time. Consider the following time-varying admittance model

$$\mathbf{M}(\mathbf{x}_a, t)\ddot{\mathbf{x}}_a + \mathbf{C}(\mathbf{x}_a, \dot{\mathbf{x}}_a, t)\dot{\mathbf{x}}_a + \mathbf{D}(\mathbf{x}_a, t)\dot{\mathbf{x}}_a + \frac{\partial P}{\partial \mathbf{x}_a}(t) = \mathbf{F}_e \quad (3)$$

where  $\mathbf{M}(\mathbf{x}_a) = \mathbf{M}^T(\mathbf{x}_a) \geq 0$  is the inertia matrix,  $\mathbf{C}(\mathbf{x}_a, \dot{\mathbf{x}}_a)$  represents the Coriolis term,  $\mathbf{D}(\mathbf{x}_a) \geq 0$  is a damping matrix and  $P: \mathbb{R}^m \rightarrow \mathbb{R}$  is a potential field acting on the system. Here, the variation of the dynamic parameters might end up introducing energy into the system, thus threatening passivity (see e.g. Secchi and Ferraguti (2019); Ferraguti et al. (2015)). The standard admittance controller cannot in fact ensure a robustly stable interaction when reproducing a time-varying dynamics.

Alongside passivity, other conditions need to be satisfied for ensuring safety during the transportation task, both for the human, the robot and the manipulated object. These conditions require a dedicated proper formulation.

We aim at realising a control architecture capable of performing a collaborative human-robot transportation task in a safe and flexible way. The architecture must be capable of passively implementing a variable admittance dynamics as in (3), whose parameters must adapt to properly assist the human operator, alongside accomplishing multiple safety-related and application-oriented tasks, while treating the mobile manipulator as a single whole-body system.

### 3. WHOLE BODY KINEMATIC MODEL

In this section we present the construction of the augmented kinematic mapping in (2).

First, we separately compute the kinematic contribution of the arm to the end-effector velocity  ${}^W\dot{\mathbf{x}}_{E(a)}$  and the contribution of the mobile base  ${}^W\dot{\mathbf{x}}_{E(b)}$ . Considering the kinematic mapping of the arm, this is readily available as:

$${}^0\dot{\mathbf{x}}_a = \mathbf{J}_a \dot{\mathbf{q}}_a \quad (4)$$

being  $\mathbf{J}_a$  the geometric Jacobian of the arm, relating the velocity of the terminating link  $\mathcal{F}_a$  w.r.t the initial link frame  $\mathcal{F}_0$  expressed in  $\mathcal{F}_0$  with the joint velocities  $\dot{\mathbf{q}}_a$ . We assume that the tool frame is related to the end tip one via a constant homogeneous transformation matrix  ${}^a\mathbf{T}_E$ , as the initial frame is related to the world frame via  ${}^W\mathbf{T}_0$ . The contribution of the manipulator to the end-effector velocity, expressed in the world frame, is obtained as:

$$\begin{aligned} {}^W\dot{\mathbf{x}}_{E(a)} &= \mathbf{J}_A \dot{\mathbf{q}}_a \\ \mathbf{J}_A &= {}^W\mathcal{T}_0 {}^E\mathcal{T}_a \mathbf{J}_a \end{aligned} \quad (5)$$

in which  ${}^W\mathcal{T}_0$  and  ${}^E\mathcal{T}_a$  are the adjoint matrices:

$${}^E\mathcal{T}_a = \begin{bmatrix} {}^a\mathbf{R}_E^T & -{}^a\mathbf{R}_E^T \times {}^a\mathbf{r}_E \\ \mathbf{0}_3 & {}^a\mathbf{R}_E^T \end{bmatrix} \quad (6)$$

$${}^W\mathcal{T}_0 = \begin{bmatrix} {}^W\mathbf{R}_0 & {}^W\mathbf{r}_0 \times {}^W\mathbf{R}_0 \\ \mathbf{0}_3 & {}^W\mathbf{R}_0 \end{bmatrix} \quad (7)$$

in which  ${}^a\mathbf{R}_E \in \mathbb{SO}(3)$  is the rotation matrix obtained from  ${}^a\mathbf{T}_E$ , with  ${}^a\mathbf{r}_E \in \mathbb{R}^3$  being the position vector of the transformation. Similarly, we can extract  ${}^W\mathbf{R}_0 \in \mathbb{SO}(3)$  and  ${}^W\mathbf{r}_0$  from  ${}^W\mathbf{T}_0$ .

For the mobile base, we utilise the kinematic mapping commonly found in literature for a differential drive robot (see e.g. LaValle (2006)). Given the choice of  $\mathbf{q}_b$ , we indicate as  $\dot{\mathbf{q}}_b = [\omega_l \ \omega_r]^T$  the angular velocity of the

left and right wheel respectively. We can then define the kinematic mapping of the mobile base as:

$${}^W\dot{\mathbf{x}}_b = \mathbf{J}_b \dot{\mathbf{q}}_b \quad (8)$$

which relates the velocity of the wheels with the Cartesian velocity of the mobile base w.r.t the world frame  $\mathcal{F}_W$  expressed in  $\mathcal{F}_W$ . The Jacobian  $\mathbf{J}_b \in \mathbb{R}^{m \times n_b}$  stems from the kinematic model of the unicycle together with the geometric parameters of the differential drive system:

$$\mathbf{J}_b = \begin{bmatrix} \frac{r \cos(\theta)}{2} & \frac{r \cos(\theta)}{2} \\ \frac{r \sin(\theta)}{2} & \frac{r \sin(\theta)}{2} \\ \mathbf{0}_{3 \times 2} & \\ \frac{r}{L} & -\frac{r}{L} \end{bmatrix} \quad (9)$$

in which  $L$  is the distance between the two wheels,  $r$  is the radius of the wheels and  $\theta$  is the steering angle of the mobile base w.r.t. the world frame  $\mathcal{F}_W$ .

The kinematic model in (8) considers as a reference point for the motion the midpoint of the wheel axis. This is however subject to non-holonomic constraints, which limit the instantaneous mobility of the robot. In order to overcome this limitation, we deploy a I-O SFL controller d'Andréa Novel et al. (1995), which allows us to linearize static state feedback laws. By shifting to a reference point located at a distance  $b$  from the wheel axis w.r.t. the base frame  $\mathcal{F}_b$ , the translational velocity of the reference control point is unrestricted. The kinematic model in (8) becomes:

$${}^W\dot{\mathbf{x}}_B = \mathbf{J}_B \dot{\mathbf{q}}_b \quad (10)$$

in which  ${}^W\dot{\mathbf{x}}_B$  is the Cartesian velocity of the new control point w.r.t the world frame  $\mathcal{F}_W$ , while the corresponding Jacobian  $\mathbf{J}_B$  is defined as:

$$\mathbf{J}_B = \begin{bmatrix} \left(\frac{r \cos \theta}{2} - \frac{br \sin(\theta)}{L}\right) & \left(\frac{r \cos \theta}{2} + \frac{br \sin(\theta)}{L}\right) \\ \left(\frac{r \sin \theta}{2} + \frac{br \cos(\theta)}{L}\right) & \left(\frac{r \sin \theta}{2} - \frac{br \cos(\theta)}{L}\right) \\ \mathbf{0}_{3 \times 2} & \\ \frac{r}{L} & -\frac{r}{L} \end{bmatrix} \quad (11)$$

Finally, we introduce a mapping term which allows us to compute the contribution to the end effector velocity due to the mobile base as:

$${}^W\dot{\mathbf{x}}_{E(b)} = \mathbb{H} \mathbf{J}_B \dot{\mathbf{q}}_b \quad (12)$$

in which  $\mathbb{H} \in \mathbb{R}^{m \times m}$  is defined as:

$$\mathbb{H} = \begin{bmatrix} 1 & 0 & 0 & 0 & 0 & -{}^B y_E \\ 0 & 1 & 0 & 0 & 0 & {}^B x_E \\ & & \mathbf{0}_{3 \times 6} & & & \\ 0 & 0 & 0 & 0 & 0 & 1 \end{bmatrix} \quad (13)$$

with  $({}^B x_E, {}^B y_E)$  being the Cartesian coordinates of the end effector with respect to the frame  $\mathcal{F}_B$ .

Merging (5) and (12) we can achieve the mapping in (2) using the augmented generalized velocities  $\dot{\mathbf{q}} = [\dot{\mathbf{q}}_b^T \ \dot{\mathbf{q}}_a^T]^T$  and by constructing the augmented Jacobian  $\mathbf{J}_m$  as:

$$\mathbf{J}_m = [\mathbb{H} \mathbf{J}_B \quad \mathbf{J}_A] \quad (14)$$

We can thus track a desired reference velocity for the robot  $\dot{\mathbf{x}}_{des} = {}^W\dot{\mathbf{x}}_{E(a)} + {}^W\dot{\mathbf{x}}_{E(b)}$  via the generalized velocities:

$$\dot{\mathbf{q}}_{des} = \mathbf{J}_m^+ \dot{\mathbf{x}}_{des} \quad (15)$$

#### 4. COLLABORATIVE CONSTRAINT-ORIENTED CONTROL ARCHITECTURE

In this section we provide the necessary tools for building the constraint-oriented control architecture proposed in Benzi and Secchi (2021), which is based on energy tanks Franken et al. (2011) and CBFs for task encoding Notomista and Egerstedt (2019). We finally present the policy for adapting the admittance parameters online.

##### 4.1 Energy Tanks

Energy tanks are energy reservoirs modelled as:

$$\begin{cases} \dot{x}_t = u_t \\ y_t = \frac{\partial T}{\partial x_t} = x_t(t) \end{cases} \quad (16)$$

where  $x_t \in \mathbb{R}$  is the state of the tank, the pair  $(u_t, y_t) \in \mathbb{R} \times \mathbb{R}$  represents the power port through which the tank exchanges energy and

$$T(x_t) = \frac{1}{2}x_t^2 \quad (17)$$

is the storage function of the energy tank.

The energy stored inside tanks is not affected by any specific dynamics, meaning that it can be purposefully utilised at any stage for performing any desired behaviour. This is carried out, in the case of the standard admittance controller in (3), by interconnecting the power port of the tank  $(u_t, y_t)$  with the power port  $(\mathbf{F}_e, \dot{\mathbf{x}}_{des})$  of the implemented admittance dynamics, via:

$$\begin{cases} u_t(t) = \dot{x}_t(t) = \mathbf{A}^T(t)\mathbf{F}_e(t) \\ \dot{\mathbf{x}}_{des}(t) = \mathbf{A}(t)y_t(t) = \boldsymbol{\gamma}(t) \end{cases} \quad (18)$$

where  $\mathbf{A}(t) \in \mathbb{R}^m$  is defined as

$$\mathbf{A}(t) = \frac{\boldsymbol{\gamma}(t)}{x_t(t)} \quad (19)$$

and  $\boldsymbol{\gamma}(t) \in \mathbb{R}^n$  is the desired value for the output  $\dot{\mathbf{x}}_{des}(t)$ , i.e. the velocity resulting from the admittance dynamics. This means that by a proper modulation of the energy flow it is possible to implement any desired port behaviour. From (16),(17) and (18) we obtain

$$\dot{T} = u_t y_t = \mathbf{A}^T(t)\mathbf{F}_e y_t = \boldsymbol{\gamma}^T \mathbf{F}_e \quad (20)$$

showing how the energy flow necessary for implementing a desired admittance dynamics is provided by the tank.

A singularity occurs in (18) whenever  $x_t(t) = 0$  due to the definition of  $\mathbf{A}(t)$ , meaning that the tank is depleted and no behavior can be performed. This issue can be faced by initializing  $x_t$  such that  $T(x_t(0)) \geq \underline{\varepsilon} > 0$  and by guaranteeing that  $T(x_t(t)) \geq \underline{\varepsilon} \forall t > 0$ , with  $\underline{\varepsilon}$  being an arbitrarily set lower bound.

In Secchi and Ferraguti (2019), it was shown that if  $T(x_t) \geq \underline{\varepsilon} \forall t \geq 0$ , then the modulated tank (18) remains passive independently of the desired output  $\boldsymbol{\gamma}(t)$ . Thus, as long as the tank is not depleted, any desired port behavior can be passively implemented by modulating the energy flow. Specifically, it is possible to reproduce any passive dynamics Giordano et al. (2013); Riggio et al. (2018).

For reproducing a non-passive dynamics, such as the time varying admittance in (3), we can exploit the previous

results for passivizing the desired behaviour. The passivity of the modulated tank can be encoded as a constraint:

$$T(x_t) \geq \underline{\varepsilon} \quad \forall t \geq 0 \quad (21)$$

Then, as in Secchi and Ferraguti (2019) and Benzi and Secchi (2021), the appropriate control input can be synthesised via the following optimization problem

$$\begin{aligned} & \underset{\dot{\mathbf{x}}_{des}}{\text{minimize}} && \|\dot{\mathbf{x}}_{des} - \dot{\mathbf{x}}_a\|^2 \\ & \text{subject to} && \int_0^t \mathbf{F}_e^T(\tau)\dot{\mathbf{x}}_{des}(\tau)d\tau \geq -T(x_t(0)) + \underline{\varepsilon} \end{aligned} \quad (22)$$

The solution of (22) provides the best passive approximation of the desired behavior  $\dot{x}_a$ , by keeping track of the energy stored in the tank. We then set  $\dot{\mathbf{x}}_{des} = \boldsymbol{\gamma}$  and utilize it to tune the modulation matrix  $\mathbf{A}(t)$  in (18). This ensures a passive energy balance even if the variation of the parameters would inject energy in the system.

A discrete-time version of (22) was proposed in Secchi and Ferraguti (2019), thus obtaining a convex formulation, for a computationally fast and simple optimization problem.

##### 4.2 Control Barrier Functions

CBFs can be formulated for enforcing multiple time varying constraints on a robot described by (2). A specific procedure was described in Notomista et al. (2020), by which both a set of tasks, both kinematic limits are modelled as dynamic constraints onto the input of the systems. These can then be inserted into an optimization problem, whose solution is the input satisfying all the constraints, i.e. leading to the simultaneous execution of all the tasks.

We represent the desired tasks as the minimization of a non-negative, time-varying, continuously-differentiable cost function  $C : \mathbb{R}^n \times \mathbb{R} \rightarrow \mathbb{R}$ . Considering a robot modelled as (2) and the time-varying task variable  $\boldsymbol{\sigma} \in \mathbb{R}^n$  as an output variable, the task execution can be encoded via the following optimization problem:

$$\begin{aligned} & \underset{\mathbf{u}}{\text{minimize}} && C(\boldsymbol{\sigma}, t) \\ & \text{subject to} && {}^W \dot{\mathbf{x}}_E = \mathbf{J}_m(\mathbf{q}) \mathbf{u} \\ & && \boldsymbol{\sigma} = \mathbf{k}({}^W \mathbf{x}_E, t) \end{aligned} \quad (23)$$

A convex formulation of the problem can be obtained by leveraging Control Barrier Functions. Let  $\mathcal{C} \subset \mathbb{R}^n$  be the subset in which the task is considered to be executed, i.e.  $C(\boldsymbol{\sigma}, t) = 0$ . Let then  $h : \mathbb{R}^n \times \mathbb{R} \rightarrow \mathbb{R}$  be a control barrier function defined as  $h(\boldsymbol{\sigma}, t) = -C(\boldsymbol{\sigma}, t)$ . We have that  $h$  is non negative only whenever  $C(\boldsymbol{\sigma}, t) = 0$ , i.e. the region of satisfaction of the task. By enforcing the non-negativity of  $h$  we can then achieve the execution of the task  $\boldsymbol{\sigma}$ . This results in the following convex optimization problem Notomista and Egerstedt (2019):

$$\begin{aligned} & \underset{\dot{\mathbf{q}}}{\text{minimize}} && \|\dot{\mathbf{q}}\|^2 \\ & \text{subject to} && \frac{\partial h}{\partial t} + \frac{\partial h}{\partial \boldsymbol{\sigma}} \frac{\partial \boldsymbol{\sigma}}{\partial {}^W \mathbf{x}_E} \mathbf{J}_m(\mathbf{q})\dot{\mathbf{q}} + \alpha(h(\boldsymbol{\sigma}, t)) \geq 0 \end{aligned} \quad (24)$$

where  $\alpha(\cdot)$  is an extended class  $\mathcal{K}$  function<sup>1</sup> and where we have chosen as an input for (2)  $\mathbf{u} = \dot{\mathbf{q}}$ .

<sup>1</sup> An extended class  $\mathcal{K}$  is a function  $\phi : \mathbb{R} \rightarrow \mathbb{R}$  such that  $\phi$  is strictly increasing and  $\phi(0) = 0$

We can straightforwardly extend the formulation in order to implement the execution of multiple  $M$  different tasks at the same time, each respectively encoded by the cost functions  $C_1, \dots, C_M$ . At the same time, we can add the passivity constraint in (22) to the stack, thus obtaining a single convex optimization problem as in Benzi and Secchi (2021). The final formulation is:

$$\begin{aligned} & \underset{\dot{\mathbf{q}}, \boldsymbol{\delta}}{\text{minimize}} && \|\dot{\mathbf{q}} - \dot{\mathbf{q}}_{adm}\|^2 + l\|\boldsymbol{\delta}\|^2 \\ & \text{subject to} && \frac{\partial h_m}{\partial t} + \frac{\partial h_m}{\partial \boldsymbol{\sigma}} \frac{\partial \boldsymbol{\sigma}}{\partial^W \mathbf{x}_E} \mathbf{J}_m(\mathbf{q}) \dot{\mathbf{q}} \\ & && + \alpha(h_m(\boldsymbol{\sigma}, t)) \geq -\boldsymbol{\delta}_m \quad m \in \{1, \dots, M\} \\ & && \int_0^t \mathbf{F}_e^T(\tau) \mathbf{J}_m(\mathbf{q}) \dot{\mathbf{q}}(\tau) d\tau \geq -T(x_t(0)) + \varepsilon \end{aligned} \quad (25)$$

in which  $\dot{\mathbf{q}}_{adm} = \mathbf{J}_m(\mathbf{q})^+ \dot{\mathbf{x}}_a$  is the desired admittance expressed in the joint space,  $h_m(\boldsymbol{\sigma}, t) = -C_m(\boldsymbol{\sigma}, t)$  and  $\boldsymbol{\delta} = [\delta_1, \dots, \delta_M]^T$  is the vector of slack variables dedicated to relaxing each constraint, while  $l \geq 0$  is a scaling factor. The slack variables  $\delta_m$  are required for ensuring the feasibility of the problem at all times, even if conflicting constraints are simultaneously active.

We have thus built an architecture capable of implementing both a passive time-varying admittance controller, both the execution of multiple tasks at the same time.

### 4.3 Admittance Parameters Adaptation

The choice of the dynamic parameters for a given admittance directly affects how the human perceives the interaction and the overall quality of the collaboration Duchaine and Gosselin (2007).

Our goal is to adapt online the admittance parameters according to his perceived intention of the operator, in order to properly assist him during the collaborative transportation task. We utilize the adaptation policy proposed in Lecours et al. (2012), where the human intention is inferred by monitoring the magnitude and the direction of the desired acceleration, alongside the current velocity value. Two possible intentions are taken into account: acceleration and deceleration. The damping and inertia parameters are updated at each cycle according to the perceived intention, starting from default values of  $\mathbf{D}_f$  and  $\mathbf{M}_f$ . The damping term  $\mathbf{D}$  is tuned as follows:

$$\begin{cases} \mathbf{D} = \mathbf{D}_f - \mathbb{I}_m \odot (\alpha_a |\ddot{\mathbf{x}}_a| \mathbf{1}_m^T) & \text{if acceleration} \\ \mathbf{D} = \mathbf{D}_f + \mathbb{I}_m \odot (\alpha_d |\ddot{\mathbf{x}}_a| \mathbf{1}_m^T) & \text{if deceleration} \end{cases} \quad (26)$$

in which  $\alpha_a$  and  $\alpha_d$  are two gains to be tuned,  $|\cdot|$  indicates the magnitude of the vector,  $\mathbb{I}_m \in \mathbb{R}^{m \times m}$  is the identity matrix,  $\mathbf{1}_m \in \mathbb{R}^m$  is the vector of ones, while  $\odot$  indicates the Hadamard (or element-wise) product. The inertia values are computed according to the damping ones, by ensuring that the ratio  $\frac{\mathbf{M}(\mathbf{x}_a)}{\mathbf{D}(\mathbf{x}_a)}$  remains proportional, resulting in a more intuitive interaction for the operator:

$$\begin{cases} \mathbf{M} = \frac{\mathbf{M}\mathbf{D}}{\mathbf{D}_f} & \text{if acceleration} \\ \mathbf{M} = \frac{\mathbf{M}}{\mathbf{D}_f} (1 - \beta(1 - e^{-\eta(\mathbf{D} - \mathbf{D}_f)})) \mathbf{D} & \text{if deceleration} \end{cases} \quad (27)$$

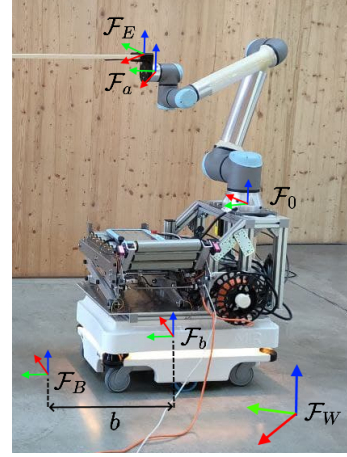


Fig. 2. Setup and structure of the mobile manipulator and frames utilized for the kinematic computations

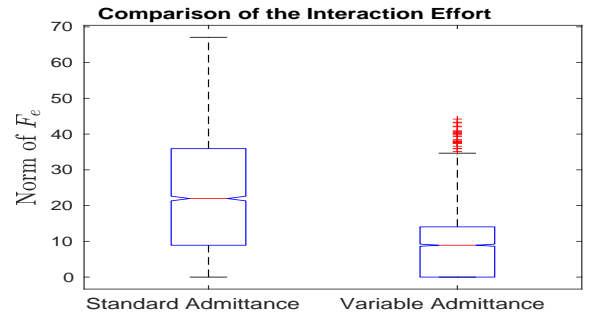


Fig. 3. Distribution over time of the force exerted by the human using the two admittance controllers

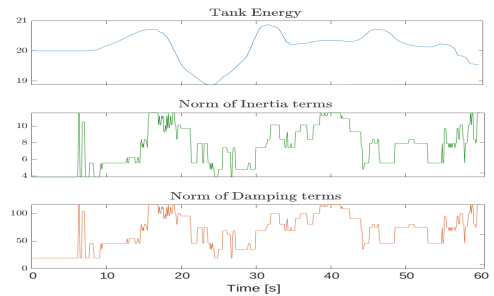


Fig. 4. Norm of the variation of the admittance parameters and evolution of the energy in the tank over time

in which  $\beta \in (0, 1)$  serves to tune the steady-state value of  $\frac{\mathbf{M}(\mathbf{x}_a)}{\mathbf{D}(\mathbf{x}_a)}$ , while  $\eta$  is a parameter defining the smoothness with which the ratio varies (see Lecours et al. (2012)).

## 5. EXPERIMENTS

An experimental evaluation has been conducted, in order to validate each individual component of the architecture. The mobile manipulator used in the validation is composed of a MiR 100 mobile base, with a 6-DOF collaborative manipulator UR10e mounted on top. In Fig. 2 the overall setup, as well as the utilized frames can be observed.

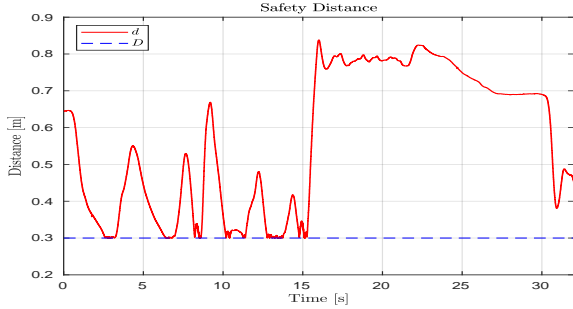


Fig. 5. Evolution of the safety distance over time.

### 5.1 Passive Time-Varying Admittance Controller

First, the collaborative transportation task is carried out, highlighting the advantages of the passive time-varying admittance controller. During the experiment, a wooden plank of  $2.5m$  in length is attached to the tool of the manipulator (see Fig. 2), while the human is holding the opposite side. As the human pulls his side of the plank, the interaction force  $\mathbf{F}_e$  is sensed by the on-board F/T sensor of the UR10e. After being transformed by means of  ${}^W\mathcal{T}_E$  into the world frame, the force is integrated via the time-varying admittance dynamics (3) for producing a desired operational velocity set-point  $\dot{\mathbf{x}}_{des}$ . By means of the whole body kinematic mapping in (15), a desired velocity for both the arm joints and the mobile base wheels is then synthesized. In this way, the robot can actively assist the human in the transportation of the load.

During the transportation task, an experienced user has to navigate in a constricting environment, with frequent stops and turns. In this scenario, the online adaptation of the admittance parameters allows to visibly enhance the quality of the interaction. In fact, by dynamically varying the mass and damping terms as shown in Sec. 4, the human is assisted while decelerating and accelerating the robot, resulting in reduced physical effort from his side. This can be observed in Fig. 3, in which the distribution of the force exerted by the operator over time using the standard and the variable admittance controller is portrayed. For the standard case, the values of inertia and damping were fixed at the default ones  $\mathbf{M}_f$  and  $\mathbf{D}_f$ , namely  $4kg$  and  $20\frac{Ns}{m}$ .

As shown in Sec. 4, the overall passivity is ensured by the energy tank and the energetic condition in (22), thus ensuring a robustly stable interaction. The variation of the dynamic parameters during the task, as well as the evolution of the energy in the tank, are portrayed in Fig. 4.

### 5.2 CBF-based tasks

Alongside the main transportation task, a set of additional secondary task is implemented. These are encoded via CBFs and inserted into the optimization problem in (25).

First, the safety of the transported object is ensured. The load is wrapped with a capsule Lin et al. (2017), a virtual object composed by two semi-spheres, centred in the two mid-points of the short edges of the plank, and a cylinder whose longitudinal axis links the two points. Then, a minimum safety distance  $D_{min} = 0.3m$  between the capsule and a detectable object in the scene is guaranteed by means of the following CBF

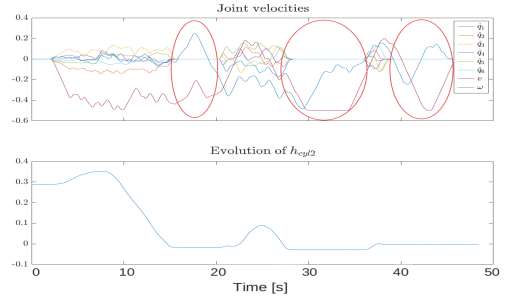


Fig. 6. Value of the augmented joint velocities and evolution of  $h_{cyl2}$  over time. Whenever  $h_{cyl2} = 0$ , only the mobile base contributes to the motion.

$$h_{safe} = d^2 - D_{min}^2 \quad (28)$$

in which the safety distance  $d \in \mathbb{R}$  is defined as

$$d = \|\mathbf{x}_{obs} - \mathbf{x}_c\| - r_c \quad (29)$$

where  $\mathbf{x}_{obs} \in \mathbb{R}^m$  is the position of the obstacle, while  $\mathbf{x}_c \in \mathbb{R}^m$  is the position on the capsule which is closest to the obstacle and  $r_c \in \mathbb{R}$  is the radius of the capsule. Given that the manipulator is significantly more dexterous than the mobile base and that sudden rotations of the base can be negatively perceived by the human, we decided to only employ the manipulator for this safety task. Thus, its execution can be performed by adding in (25) the constraint:

$$2(\mathbf{x}_{obs} - \mathbf{x}_c)^T \mathbf{J}_{lim} \dot{\mathbf{q}} \geq -\alpha(h_{safe}) + \delta_{safe} \quad (30)$$

with  $\mathbf{J}_{lim} = [\mathbf{0}_{6 \times 2}^T \mathbf{J}_a^T]^T$  being the restriction of the augmented Jacobian to the manipulator alone. The plot in Fig 5 portrays the evolution of  $d$  over time, showing how the safety distance is always respected.

This procedure can be extended for guaranteeing the safety of the overall structure by wrapping with capsules the entire system.

Additionally, we restrict the workspace of the manipulator to a suitable subset for the application. First, in order to avoid self collision between the tool mounted onto the manipulator and its joints, we define the following CBF

$$h_{cyl1} = d_1^2 - R_1^2 \quad (31)$$

with  $d_1 = \sqrt{{}^0x_{E1}^2 + {}^0x_{E2}^2}$  and  $R_1$  being the radius which defines a safety cylinder centred in the manipulator base.

Additionally, we want to limit the outreach of the manipulator, in order to avoid singularities during the transportation, as they could lead to unexpected behaviours. We then deploy the following CBF for forcing the tip of the manipulator to stay inside a set cylinder of radius  $R_2$

$$h_{cyl2} = -d_1^2 + R_2^2 \quad (32)$$

Fig. 6 shows the contribution of this CBF; as the manipulator reaches the edge of the cylinder, its joint velocities halt, restarting only as it recoils in the desired area.

## 6. CONCLUSIONS AND FUTURE WORKS

In this paper we developed a control architecture capable of performing a flexible and robust collaborative transportation task, treating the mobile manipulator as a whole-body system and considering non-holonomic constraints. In future works, we aim at further exploiting the redundancy of the robot, for maximizing performance and compliance.

## REFERENCES

- Agravante, D.J., Cherubini, A., Bussy, A., and Kheddar, A. (2013). Human-humanoid joint haptic table carrying task with height stabilization using vision. In *2013 IEEE/RSJ International Conference on Intelligent Robots and Systems*, 4609–4614. IEEE.
- Ames, A.D., Coogan, S., Egerstedt, M., Notomista, G., Sreenath, K., and Tabuada, P. (2019). Control barrier functions: Theory and applications. In *2019 18th European Control Conference (ECC)*, 3420–3431. IEEE.
- Benzi, F., Ferraguti, F., Riggio, G., and Secchi, C. (2022). An energy-based control architecture for shared autonomy. *IEEE Transactions on Robotics*, 1–19. doi:10.1109/TRO.2022.3180885.
- Benzi, F. and Secchi, C. (2021). An optimization approach for a robust and flexible control in collaborative applications. In *2021 IEEE International Conference on Robotics and Automation (ICRA)*, 3575–3581. IEEE.
- Calinon, S., Evrard, P., Gribovskaya, E., Billard, A., and Kheddar, A. (2009). Learning collaborative manipulation tasks by demonstration using a haptic interface. In *2009 International Conference on Advanced Robotics*, 1–6. IEEE.
- Calinon, S., Guenter, F., and Billard, A. (2007). On learning, representing, and generalizing a task in a humanoid robot. *IEEE Transactions on Systems, Man, and Cybernetics, Part B (Cybernetics)*, 37(2), 286–298.
- d’Andréa Novel, B., Campion, G., and Bastin, G. (1995). Control of nonholonomic wheeled mobile robots by state feedback linearization. *The International journal of robotics research*, 14(6), 543–559.
- Dimeas, F. and Arapagathos, N. (2016). Online stability in human-robot cooperation with admittance control. *IEEE transactions on haptics*, 9(2), 267–278.
- Duchaine, V. and Gosselin, C.M. (2007). General model of human-robot cooperation using a novel velocity based variable impedance control. In *Second Joint Euro-Haptics Conference and Symposium on Haptic Interfaces for Virtual Environment and Teleoperator Systems (WHC’07)*, 446–451. IEEE.
- Ferraguti, F., Preda, N., Manurung, A., Bonfe, M., Lambercy, O., Gassert, R., Muradore, R., Fiorini, P., and Secchi, C. (2015). An energy tank-based interactive control architecture for autonomous and teleoperated robotic surgery. *IEEE Transactions on Robotics*, 31(5), 1073–1088.
- Ferraguti, F., Talignani Landi, C., Sabattini, L., Bonfè, M., Fantuzzi, C., and Secchi, C. (2019). A variable admittance control strategy for stable physical human-robot interaction. *The International Journal of Robotics Research*, 38(6), 747–765.
- Ferrari, D., Benzi, F., and Secchi, C. (2022). Bidirectional communication control for human-robot collaboration. In *2022 International Conference on Robotics and Automation (ICRA)*, 7430–7436. doi:10.1109/ICRA46639.2022.9811665.
- Franken, M., Stramigioli, S., Misra, S., Secchi, C., and Macchelli, A. (2011). Bilateral telemanipulation with time delays: A two-layer approach combining passivity and transparency. *IEEE transactions on robotics*, 27(4), 741–756.
- Giordano, P.R., Franchi, A., Secchi, C., and Bühlhoff, H.H. (2013). A passivity-based decentralized strategy for generalized connectivity maintenance. *The International Journal of Robotics Research*, 32(3), 299–323. doi:10.1177/0278364912469671.
- Gribovskaya, E., Kheddar, A., and Billard, A. (2011). Motion learning and adaptive impedance for robot control during physical interaction with humans. In *2011 IEEE International Conference on Robotics and Automation*, 4326–4332. IEEE.
- Hersch, M., Guenter, F., Calinon, S., and Billard, A. (2008). Dynamical system modulation for robot learning via kinesthetic demonstrations. *IEEE Transactions on Robotics*, 24(6), 1463–1467.
- LaValle, S.M. (2006). *Planning Under Differential Constraints*, 587–589. Cambridge University Press. doi:10.1017/CBO9780511546877.016.
- Lecours, A., Mayer-St-Onge, B., and Gosselin, C. (2012). Variable admittance control of a four-degree-of-freedom intelligent assist device. In *2012 IEEE international conference on robotics and automation*, 3903–3908. IEEE.
- Lin, H.C., Liu, C., Fan, Y., and Tomizuka, M. (2017). Real-time collision avoidance algorithm on industrial manipulators. In *2017 IEEE Conference on Control Technology and Applications (CCTA)*, 1294–1299. IEEE.
- Notomista, G. and Egerstedt, M. (2019). Constraint-driven coordinated control of multi-robot systems. In *2019 American Control Conference (ACC)*, 1990–1996. IEEE.
- Notomista, G. and Egerstedt, M. (2020). Persistification of robotic tasks. *IEEE Transactions on Control Systems Technology*.
- Notomista, G., Mayya, S., Selvaggio, M., Santos, M., and Secchi, C. (2020). A set-theoretic approach to multi-task execution and prioritization. In *2020 IEEE International Conference on Robotics and Automation (ICRA)*, 9873–9879. IEEE.
- Nozaki, K. and Murakami, T. (2009). A motion control of two-wheels driven mobile manipulator for human-robot cooperative transportation. In *2009 35th Annual Conference of IEEE Industrial Electronics*, 1574–1579. IEEE.
- Riggio, G., Fantuzzi, C., and Secchi, C. (2018). On the use of energy tanks for multi-robot interconnection. In *2018 IEEE/RSJ International Conference on Intelligent Robots and Systems (IROS)*, 3738–3743. IEEE.
- Secchi, C. and Ferraguti, F. (2019). Energy optimization for a robust and flexible interaction control. In *2019 International Conference on Robotics and Automation (ICRA)*, 1919–1925. IEEE.
- Secchi, C., Stramigioli, S., and Fantuzzi, C. (2007). *Control of interactive robotic interfaces: A port-Hamiltonian approach*, volume 29. Springer Science & Business Media.
- Siciliano, B. and Villani, L. (2012). *Robot force control*, volume 540. Springer Science & Business Media.
- Tagliabue, A., Kamel, M., Verling, S., Siegwart, R., and Nieto, J. (2017). Collaborative transportation using mavs via passive force control. In *2017 IEEE international conference on robotics and automation (ICRA)*, 5766–5773. IEEE.